Second harmonic generation on incommensurate structures: The case of multiferroic $MnWO_4$

D. Meier, N. Leo, G. Yuan, Th. Lottermoser, and M. Fiebig
Helmholtz-Institut für Strahlen-und Kernphysik, Universität Bonn, Nussallee 14-16, 53115 Bonn, Germany

P. Becker and L. Bohatý
Institut für Kristallographie, Universität zu Köln, Zülpicher Strasse 49b, 50674 Köln, Germany
(Received 16 August 2010; published 7 October 2010)

A comprehensive analysis of optical second harmonic generation on an incommensurate (IC) magnetically ordered state is presented using multiferroic $MnWO_4$ as model compound. Two fundamentally different SHG contributions coupling to the primary IC magnetic order or to secondary commensurate projections of the IC state, respectively, are distinguished. Whereas the latter can be described within the formalism of the 122 commensurate magnetic point groups the former involves a breakdown of the conventional macroscopic symmetry analysis because of its sensitivity to the lower symmetry of the *local environment* in a crystal lattice. Our analysis thus foreshadows the fusion of the hitherto disjunct fields of nonlinear optics and IC order in condensed-matter systems.

DOI: 10.1103/PhysRevB.82.155112 PACS number(s): 42.65.Ky, 61.44.Fw, 75.85.+t, 78.67.−n

I. INTRODUCTION: IMAGING INCOMMENSURATE ORDER

A crystal structure is called incommensurate (IC), if a periodic deviation of atomic parameters from the basic crystal structure cannot be related to the periodicity of the underlying crystal structure by a rational number.[1] The violation of the translation symmetry of the basic crystal structure by the IC long-range order manifests in an astonishing diversity of unusual physical effects so that systems with IC phases attracted a lot of attention since Dehlinger reported the first aperiodic crystal in 1927.[2] Nowadays, IC order is known to play an essential role in quasicrystals,[3] liquid crystals,[4] magnetic multilayers,[5] or polymers.[6] Other examples for the omnipresence of IC phases can be found among systems with strong electronic correlations such as high-temperature superconductors,[7] colossal-magnetoresistance manganites,[8] or multiferroics.[9] The pronounced reduction of symmetry by the IC order reflects the complexity of the underlying microscopic interactions. Macroscopically, this can lead to a variety of phases that become allowed in the IC state[10] and enrich the phase diagram of the host material—a key ingredient for the design of multifunctional materials.

Despite the longstanding interdisciplinary interest in IC structures, their theoretical and experimental analysis is still a challenge. For instance, it was realized only recently that an IC magnetic spiral may induce a spontaneous electric polarization and a controversial discussion about the microscopic mechanisms of this coupling is persisting.[11–13] For analyzing the order parameters and domain structures of an IC structure, a group-theoretical approach based on Landau theory of phase transitions is usually chosen. A description of the IC state in a superspace with more than three dimensions[14] or, alternatively, by considering the irreducible representations of the three-dimensional space group in the presence of a modulated structure[15] are possible. Experimentally, neutron and x-ray diffraction are usually employed for investigating aperiodic spin, charge, or lattice modulations. Yet, although these established techniques constitute a versatile tool for probing IC structures, essential ingredients characterizing the IC state remain inaccessible. In particular, this applies to the domains associated to the IC state. On the one hand, the spatial resolution of a diffraction experiment is often limited because of the integrating nature of the experiment. On the other hand, most of the IC magnetic structures do not carry a macroscopic magnetization so that it is difficult to couple to the order parameter and its spatial distribution. However, since domains and domain walls determine many macroscopic physical properties and, thus, the technological feasibility of a compound, access to these domains in a convenient way is highly desirable, particularly because it is expected that the IC nature of the ordered state will lead to domains with novel properties.

A technique with inherent spatial resolution and access even to "hidden" ordered structures is optical second harmonic generation (SHG).[16] For decades SHG has been applied to image structural, magnetic, or electric domains and to reveal spatial correlation effects between them.[17–19] More recently, SHG was even used to resolve the subpicosecond dynamics of a magnetic order parameter.[20,21] However, almost any form of long-range order probed by SHG thus far was commensurate. In the very small number of investigations on IC structures it was demonstrated that the emergence of the IC state is reflected by changes in the SHG yield but a theoretical analysis of the detected signal was never attempted.[22–25] The same holds for recent investigations on IC magnetic ferroelectrics where SHG was used for imaging magnetic and ferroelectric domains without performing a detailed discussion of the SHG contributions and the IC symmetries involved.[26,27] Thus, a resilient framework categorizing the nonlinear interactions between the electromagnetic light fields and an aperiodically ordered state of matter is yet to be developed.

In this paper we present a comprehensive analysis of optical SHG on an IC magnetically ordered state. Using multiferroic $MnWO_4$ as model compound, two principally different SHG contributions coupling to the symmetry-breaking order parameters are identified. The first one corresponds to a commensurate projection of the IC magnetic state that is represented by an improper order parameter and can be de-

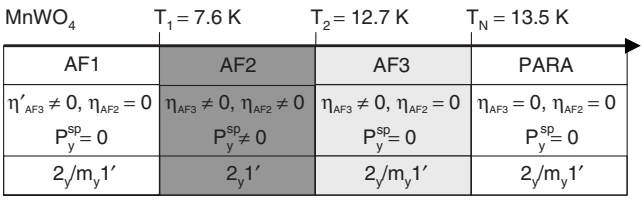

FIG. 1. Overview of the magnetic phases (Refs. 35 and 36), the symmetry-breaking order parameters (Refs. 33 and 34), and the corresponding commensurate point groups for multiferroic $MnWO_4$.

scribed within the 122 commensurate magnetic point groups. The second one reflects the entire IC structure of the compound and involves a breakdown of the conventional macroscopic symmetry analysis since local symmetries become involved. With our analysis we foreshadow the fusion of the hitherto disjunct fields of nonlinear optics and IC order in condensed-matter systems.

II. INCOMMENSURATE ORDER IN MULTIFERROIC $MnWO_4$

Multiferroics are compounds uniting at least two primary forms of (anti-) ferroic order in the same phase of a material. The majority of research activities is devoted to the magnetically ordered ferroelectrics since the coexistence of magnetic and electric order is a potential source for magnetoelectric cross correlations allowing one to manipulate magnetic order by electric fields (or vice versa). The most pronounced, so-called "gigantic," magnetoelectric coupling effects are observed when IC magnetic order promotes the emergence of a spontaneous electric polarization that is rigidly coupled to the magnetic order parameter. Because of the novel and unusual nature of this manifestation of IC order and the intense desire to advance our understanding of it, the choice of an IC magnetically induced ferroelectric as model system for unraveling the relation between IC order and SHG suggests itself.

We select $MnWO_4$ because it combines a relatively simple crystallograhic structure with a variety of IC phases. The magnetic phase diagram is well established and the general feasibility of an approach by SHG has already been demonstrated[26–28] so that we can now focus on analyzing the correlation between SHG and the IC state. $MnWO_4$ is closely related to compounds such as $TbMnO_3$, $Ni_2V_3O_8$, or CuO (Refs. 29–31) so that the results gained here will be of general use.

The multiferroic phase of $MnWO_4$ is governed by two fundamentally different types of order parameters: (i) a set of two primary magnetic order parameters (η_{AF3}, η_{AF2}) and (ii) one secondary electric order parameter (P_y^{sp}). The sequence of phase transitions leading to the two classes of order parameters in $MnWO_4$ is sketched in Fig. 1. Below $T_N = 13.5$ K the magnetic moments of Mn^{2+} align in a collinear way along the easy axis while their magnitudes are sinusoidally modulated with $\mathbf{k}_{AF3}=(-0.214, \frac{1}{2}, 0.457)$.[32] The resulting IC spin-density wave breaks the translation symmetry of the lattice but conserves the inversion symmetry of the crystal. This so-called AF3 phase can be described by a single two-dimensional magnetic order parameter $\eta_{AF3} = (\sigma_{AF3}e^{i\theta_{AF3}}, \sigma_{AF3}e^{-i\theta_{AF3}})$.[33,34] Upon further cooling an additional transverse spin component orders at $T_2 = 12.7$ K. In this AF3 $\rightarrow$ AF2 transition the spin-density wave turns into an elliptical spin spiral without changing the IC periodicity of the modulation so that $\mathbf{k}_{AF2}=\mathbf{k}_{AF3}$. The AF3 $\rightarrow$ AF2 transition is driven by a second magnetic order parameter $\eta_{AF2} = (\sigma_{AF2}e^{i\theta_{AF2}}, \sigma_{AF2}e^{-i\theta_{AF2}})$. The coexistence of η_{AF2} and η_{AF3} breaks the inversion symmetry and induces a spontaneous polarization P_y^{sp} along the y axis $(y \| b)$ according to[33–37]

$$P_y^{sp} \propto \sigma_{AF2}\sigma_{AF3} \tag{1}$$

thus constituting the multiferroic phase of $MnWO_4$. The correlation expressed by Eq. (1) implies that the IC nature of the primary (proper) order parameters η_i with amplitudes σ_i is projected onto the secondary (improper; here: pseudoproper[33]) order parameter P_y^{sp}. The projection corresponds to a commensurate net polarization that may be additionally modulated in an IC way around its net value.[33] Note that the incommensurability of P_y^{sp} is not mandatory and, even if present, remains mostly unnoticed because experimental techniques probing the spontaneous polarization such as pyroelectric measurements measure the commensurate contribution only. Macroscopically the polarized state can be therefore described by the point-group formalism used for commensurate structures, as in the lower part of Fig. 1.

At $T_1 = 7.6$ K a first-order transition to the AF1 phase with collinear spin alignment along the easy axis occurs. Along with this, the magnetic order of $MnWO_4$ becomes commensurate with $k_{AF1}=(\pm\frac{1}{4}, \frac{1}{2}, \frac{1}{2})$. As a consequence, η_{AF2} vanishes along with P_y^{sp}. The remaining order parameter is denoted as η'_{AF3} in order to emphasize its emergence from η_{AF3}.

III. OPTICAL SECOND HARMONIC GENERATION

An experimental method that is known to be particularly sensitive to the point symmetry of a crystal is optical SHG.[16] It is described by the equation[38]

$$S_i(2\omega) = \varepsilon_0 \chi_{ijk} E_j(\omega) E_k(\omega). \tag{2}$$

An electromagnetic light field $\mathbf{E}$ at frequency ω is incident on a crystal, driving a charge oscillation $\mathbf{S}(2\omega)$, which acts as source of a frequency-doubled light wave of the intensity $I_{SHG} \propto |\mathbf{S}(2\omega)|^2$. The source term $\mathbf{S}$ can be written as multipole expansion

$$\mathbf{S}(2\omega) = \mu_0 \frac{\partial^2 \mathbf{P}(2\omega)}{\partial t^2} + \mu_0 \left[\nabla \times \frac{\partial \mathbf{M}(2\omega)}{\partial t} \right] - \mu_0 \left[\frac{\partial^2 (\nabla \hat{Q})}{\partial t^2} \right] \tag{3}$$

with $\mathbf{P}(2\omega)$, $\mathbf{M}(2\omega)$, and $\nabla\hat{Q}(2\omega)$ as electric-dipole (ED), magnetic-dipole (MD), and electric-quadrupole (EQ) contributions, respectively. The nonlinear susceptibility χ_{ijk} couples incident light fields with polarizations j and k to a SHG wave with polarization i. According to Neumann's

TABLE I. Nonzero SHG tensor components χ_{ijk} allowed on the basis of a symmetry analysis within the 122 magnetocrystalline point groups (Ref. 39). The SHG tensor is related to a Cartesian reference system (x,y,z) as defined in Ref. 37. Note that SHG contributions with $i \neq j \neq k$ cannot be detected with light propagating along x, y, or z so that they are omitted. MD-SHG and EQ-SHG lead to the same selection rules and are therefore not distinguished.

Point group	Incident light	MD/EQ-SHG contributions	ED-SHG contributions
$2_y/m_y1'$	$k\|x$	$\chi^{MD,EQ}_{yyy}$, $\chi^{MD,EQ}_{yzz}$, $\chi^{MD,EQ}_{zyz}$	
(AF3, AF1)	$k\|y$		
	$k\|z$	$\chi^{MD,EQ}_{yyy}$, $\chi^{MD,EQ}_{yxx}$, $\chi^{MD,EQ}_{xyx}$	
$2_y1'$	$k\|x$	$\chi^{MD,EQ}_{yyy}$, $\chi^{MD,EQ}_{yzz}$, $\chi^{MD,EQ}_{zyz}$	χ^{ED}_{yyy}, χ^{ED}_{yzz}, χ^{ED}_{zyz}
(AF2)	$k\|y$		
	$k\|z$	$\chi^{MD,EQ}_{yyy}$, $\chi^{MD,EQ}_{yxx}$, $\chi^{MD,EQ}_{xyx}$	χ^{ED}_{yyy}, χ^{ED}_{yxx}, χ^{ED}_{xyx}

principle the symmetry of a compound determines the set of nonzero components χ_{ijk}.[16,39] As a consequence, ED-SHG vanishes in centrosymmetric media while MD-SHG and EQ-SHG remain allowed.[38]

Using Eqs. (2) and (3) and applying symmetry-dependent selection rules[39] the tensor components summarized in Table I are derived as contributions to SHG in $MnWO_4$. Note that Table I is based on the use of point groups as in Fig. 1. This is based on the assumption that translation operations and translation symmetries can be neglected in optical experiments since they are not resolved by the light. More quantitatively, the variation in the electromagnetic amplitude of the light field across the expansion of a unit cell (as limit of the nonprimitive lattice translations) is considered to be small enough to be neglected. With respect to Table I this means that the aperiodic nature of the order parameters with their violation of the translation symmetry is also not taken into account. The corresponding SHG light will be termed commensurate (C-) SHG in the following in order to emphasize that averaged, lattice-periodic properties are considered. Table I reveals that for light fields propagating along the y axis $(k\|y)$ SHG is forbidden in all phases. For $k\|x$ or $k\|z$ MD-SHG and EQ-SHG can occur at any temperature whereas ED-SHG is restricted to the multiferroic AF2 phase.

A detailed discussion of the technical aspects of SHG in ferroic systems including the experimental setup used here is found in Refs. 16 and 26. In the present experiment, melt-grown $MnWO_4$ single crystals[40] were processed into sets of polished platelets with a thickness of about 100 μm with each of the samples being oriented perpendicular to the one of the Cartesian axes x, y, and z.[37] The samples were illuminated at normal incidence in a transmission setup by light pulses of 2–5 mJ and 3–8 ns at a repetition rate of 10–40 Hz.

IV. EXPERIMENTAL RESULTS AND DISCUSSION

Based on Table I the experiments will proceed as follows: (a) identification of electronic transitions in the optical range and of any SHG contributions not coupling to magnetic or electric long-range order; (b) identification and analysis of C-SHG contributions; and (c) identification and analysis of IC-SHG contributions.

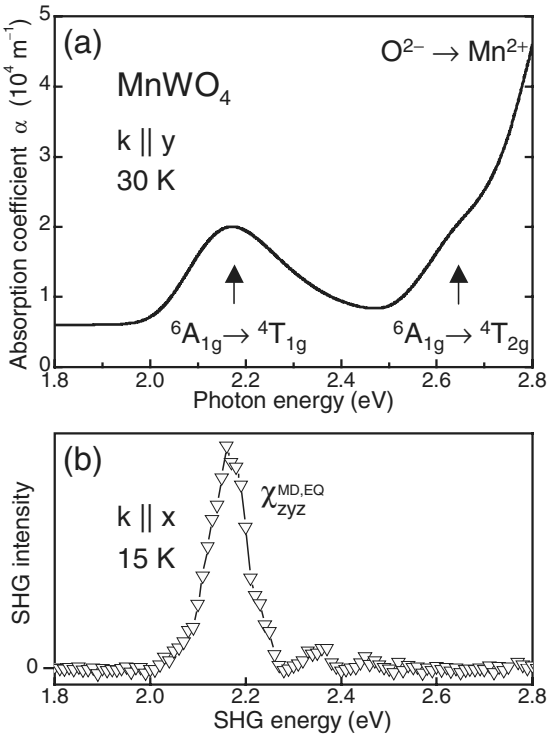

FIG. 2. Optical transitions and paramagnetic SHG contributions in $MnWO_4$. (a) Linear absorption spectrum of $MnWO_4$ obtained with x-polarized light propagating along the y axis of the crystal. At low temperature two intra-atomic and one charge-transfer transitions are identified, and labeled accordingly. (b) SHG spectra obtained in the paramagnetic phase with light incident along the x axis. Only crystallographic SHG from $\chi^{MD,EQ}_{zyz}$ is observed.

A. Optical transitions and paramagnetic SHG contributions

For identifying the electronic transitions of the Mn^{2+} ion and the crystallographic background contributions to SHG, Fig. 2 shows linear absorption spectra and polarization-dependent SHG spectra in the paramagnetic phase of $MnWO_4$. The absorption spectrum taken with x-polarized light incident along the y axis exhibits a steep increase beyond 2.7 eV which corresponds to the lowest O^{2-}–Mn^{2+} charge transfer.[41,42] In addition, absorption peaks with a width in the order of 0.1 eV are observed and marked by black arrows in Fig. 2(a). These peaks at 2.18 and 2.65 eV are assigned to the intra-atomic ${}^6A_{1g} \rightarrow {}^4T_{1g}$ and ${}^6A_{1g} \rightarrow {}^4T_{2g}$ transitions between the $Mn^{2+}(3d^5)$ orbitals.[43]

In agreement with the symmetry analysis ED-SHG contributions were not observed above T_N. The signal in Fig. 2(b) shows the ${}^6A_{1g} \rightarrow {}^4T_{1g}$ transition and is attributed to the $\chi^{MD,EQ}_{zyz}$ component, i.e., to a crystallographic C-SHG signal according to Table I. Note that out of the six components $\chi^{MD,EQ}_{ijk}$ that are allowed $\chi^{MD,EQ}_{zyz}$ is the only one that was actually observed. Its occurrence is limited to the (100) sample where it was suppressed henceforth by setting the polarization of the incident light along y or z but not in between.

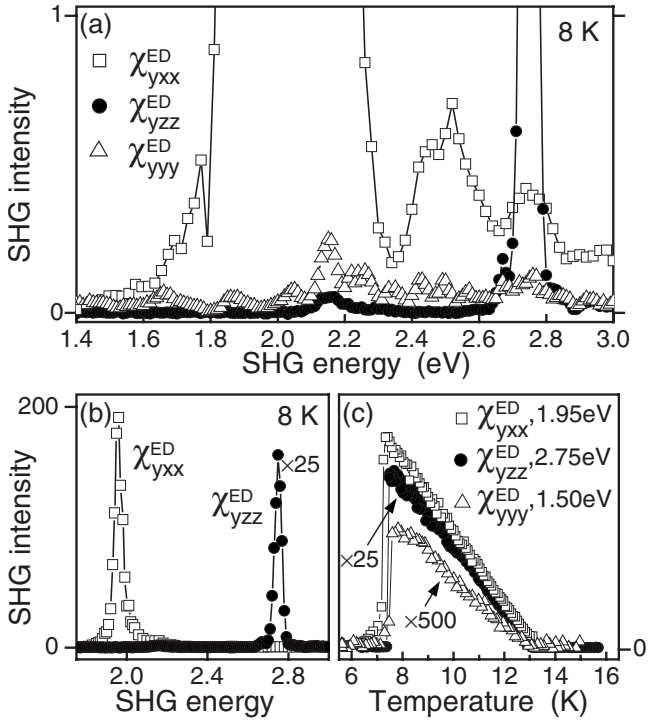

FIG. 3. Commensurate SHG in the multiferroic phase of $MnWO_4$. [(a) and (b)] C-SHG spectra obtained with $k\|x$ ($\chi^{ED}_{yzz}, \chi^{ED}_{yyy}$) and $k\|z$ (χ^{ED}_{yxx}). The exceptionally large signal yield at 1.95 eV is due to multiferroic phase matching. (c) Temperature dependence of the SHG intensity from χ^{ED}_{yzz}, χ^{ED}_{yxx}, and χ^{ED}_{yyy}. Since the latter component is quite weak it was measured at a photon energy where SHG yield from the other SHG tensor components have a comparable magnitude so that admixtures to the χ^{ED}_{yyy} are small enough to be neglected. All the signals are associated to ED-SHG contributions that are present in the multiferroic AF2 phase only. Note that the same arbitrary scale is used for the SHG intensity in Figs. 3 and 4.

B. Commensurate SHG contributions

Figure 3 shows the SHG spectra on a (100) and a (001) sample in the multiferroic AF2 phase at 8 K. Rich spectra showing all the transitions in Fig. 2(a) are observed. We identify χ^{ED}_{yyy}, χ^{ED}_{yzz}, and χ^{ED}_{yxx}. According to Table I the observed SHG contributions reflect the change in point symmetry from $2_y/m_y1'$ to $2_y1'$ by the emergence of the spontaneous polarization. The assignment is corroborated by temperature dependent measurements in Fig. 3(c). The ED-SHG contributions in Fig. 3 are nonzero only when $P^{sp}_y \neq 0$. All contributions behave according to $\chi^{ED}_{ijk} \propto P^{sp}_y$ which, because of $P^{sp}_y \propto (T_{AF2}-T)^{1/2}$ and $I_{SHG} \propto |P^{sp}_y|^2$, leads to a linear temperature dependence of the SHG intensity in the AF2 phase. At the AF2→AF1 transition the ED-SHG contributions is quenched along with the drop of P_y to zero and the reversal of the point symmetry from $2_y1'$ to $2_y/m_y1'$.

We thus see that in spite of the IC magnetic order of $MnWO_4$ the SHG signal can be fully understood on the basis of the macroscopic point group symmetries thus far. The SHG signal picks up the magnetically induced spontaneous net polarization as commensurate projection of the IC spin order while SHG contributions coupling to the underlying IC magnetic structure are not detected. Neither the polarization-dependent nor the temperature-dependent SHG measurements exhibit peculiarities revealing the presence of an aperiodic phase.

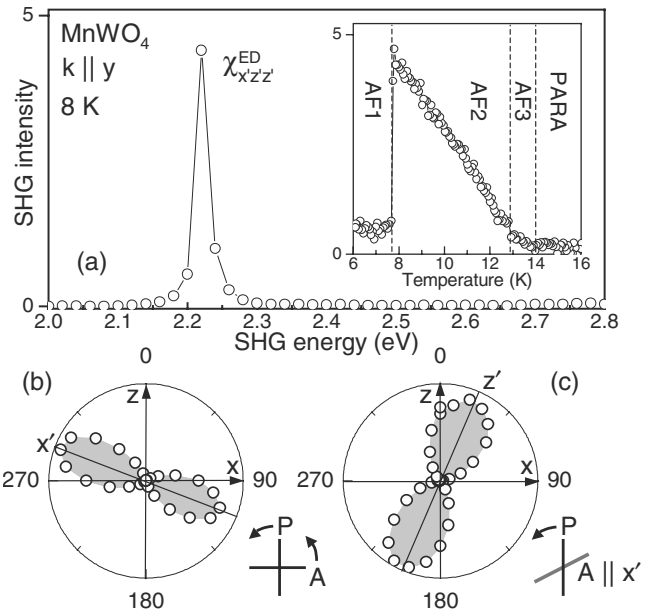

FIG. 4. Incommensurate SHG in the magnetically ordered phases of $MnWO_4$. (a) IC-SHG spectra obtained with $k\|y$ for which C-SHG contributions of any multipole order are not allowed. The temperature dependence in the inset reveals that IC-SHG is present in all three magnetic phases (and in the paramagnetic state, see text). [(b) and (c)] Polarization dependence of the IC-SHG signal at 8 K and 2.22 eV for light incident parallel to the y axis. x' and z' denote the axes of the rotated coordinate system defined by the polarization dependence of the IC-SHG signal. P and A denote the polarization of the incident light and of the detected SHG component, respectively. In (b) P and A are rotated simultaneously while in (c) P is rotated while A remains constant.

Another noteworthy issue in Fig. 3(b) is the exceptionally pronounced resonance of the χ^{ED}_{yxx} component which is due to phase matching.[38] Nearly noncritical type-I phase matching can be realized in $MnWO_4$ for incidence along x at 1.95 eV, as can be seen from the refractive indices of the crystal.[40] This constitutes a rare example of phase matching activated by magnetic order and, because of the associated spontaneous polarization, presumably the first occurrence ever of "multiferroic phase matching."

C. Incommensurate SHG contributions

Figure 4 shows the SHG spectrum obtained on a (010) sample in the multiferroic AF2 phase at 8 K with $k\|y$. A SHG signal from the ${}^6A_{1g} \rightarrow {}^4T_{1g}$ transition with a variety of most unusual properties is observed. First, the SHG yield is comparable to the commensurate SHG signals although SHG of ED, MD, and EQ type is forbidden if the macroscopic point symmetries $2_y/m_y1'$ or $2_y1'$ of Table I are applied. Second, the temperature dependence reveals that in contrast to Fig. 3(c) small SHG signals are present above T_N and in the nonmultiferroic AF3 and AF1 phases. Third, the polarization dependent data in Figs. 4(b) and 4(c) reveals lobes

consistent with a coordinate system that is rotated by about 25° around the y axis of the Cartesian system. Because of the violation of the inversion symmetry in the AF2 phase, the observed SHG contribution assigned to an ED process. The corresponding susceptibility is $\chi^{ED}_{x'z'z'}$ if the rotated coordinate system (x',y',z') shown in Fig. 4 is applied. Note that the axes x' and z' do not only deviate from the x and y axes but also from magnetic easy or hard axis.[32] We speculate that the rotation may be related to the direction perpendicular to the planes defined by the IC propagation vector $\mathbf{k}_{AF3}$. This direction includes an angle of 28° with the x axis. All the aforementioned inconsistencies suggest to associate the "forbidden" SHG signal in Fig. 4 to the IC magnetic order which has not yet been included into the symmetry analysis. This will be discussed in the following.

Remember that for a symmetry analysis as in Table I only *global* symmetries are considered. Site symmetries, defects, and translations, i.e., *local* properties that are spatially confined to the extension of the unit cell, are neglected so that only the point symmetry of a crystal is considered. For SHG experiments in the optical range this is a reasonable approximation because the wavelength of the probe light exceeds the extension of the unit cell by three orders of magnitude. However, IC phases are characterized by structural modulations *exceeding* the extension of the unit cell. Therefore the spatial variation in the electromagnetic light field across one period of the IC wave vector may no longer be negligible so that the light begins to sense the *local* symmetry of the IC structure.[44]

Based on the Neumann principle observation of SHG from $\chi^{ED}_{x'z'z'}$ indicates the presence of a local symmetry lower than $2_y1'$. Here, the only matching point group is $11'$. This becomes reasonable once the local magnetic and crystallographic structure of $MnWO_4$ is considered. The spatial variation of the electromagnetic light field couples to the local violation of the twofold rotation symmetry 2_y due to the IC nature of the ellipsoidal magnetic spin wave in the AF2 phase and leads to the reduction of the local symmetry from $2_y1'$ to $11'$. As a consequence, all components of χ^{ED}_{ijk} become symmetry allowed.

Figure 5 illustrates the violation of the local symmetry by IC order. A section whose extension is determined by the coherence length of the SHG process is considered so that any SHG light generated in the crystal section contributes coherently to the SHG yield. Figure 5(a) shows a commensurably modulated chain of atoms. One can see that the commensurate modulation conserves the symmetry axis 2_y that is indicated by the twofold rotation axis in the sketch. In contrast, the IC modulation in Fig. 5(b) violates the lattice periodicity and destroys the rotational symmetry within the considered section. Hence, locally, i.e., in the finite section probed coherently by the SHG process, the 2_y symmetry is lost.

In a similar way we can understand the SHG contribution of the paramagnetic and the AF3 and AF1 phases in the inset of Fig. 4(a). Once the IC magnetic phase is encountered it imprints a structural IC modulation with $2\mathbf{k}_{AF3}=(-0.428,1,0.914)$ onto the lattice which remains even when the IC magnetic phase is left.[45] The IC structural

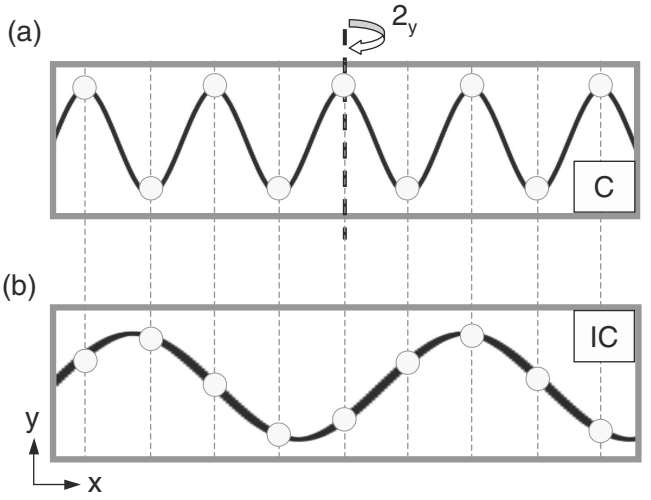

FIG. 5. Model explaining the presence of "forbidden" SHG contributions in crystals with IC order. (a) A commensurate modulation of the crystal structure retains the twofold axis of the structure. (b) An IC modulation violates the twofold symmetry locally. Additional SHG contributions may therefore emerge.

modulation lowers the local symmetry and gives rise to a small crystallographic IC contribution $\chi^{ED}_{x'z'z'}$. The slight enhancement of this signal in the AF3 and AF1 phases is most likely due to changes in the linear optical properties below T_N.[46]

The occurrence of IC-SHG contributions is reminiscent of the emergence of SHG in relaxor ferroelectrics where polar clusters reduce the local symmetry of an otherwise centrosymmetric lattice.[47,48] However, in the relaxor ferroelectrics the local perturbations are randomly distributed so that the local SHG contributions add up incoherently. In contrast, the local symmetry reduction by the IC order obeys the periodicity of the propagation vector so that the IC-SHG results from a coherent superposition. Because of this, the SHG light from adjacent magnetic translation domains related to the IC order yields a well-defined phase difference.[27]

V. CONCLUSION

In conclusion, we have analyzed the coupling of optical SHG to an incommensurately ordered state using multiferroic $MnWO_4$ as model compound. Two principally different SHG contributions coupling to the IC order parameters were identified. The first one couples to a commensurate projection of the IC state and is typically represented by a secondary, induced order parameter. This SHG contribution can be understood on the basis of a point symmetry analysis for commensurate structures and is indistinguishable from SHG contributions induced by primary commensurate order obeying the same point symmetry. The second SHG contribution couples to the primary IC order. It reflects the local symmetry of the crystal on the length scale of the IC modulation. Since the IC order breaks local symmetries, additional SHG contributions that are forbidden by the global point group symmetry of the infinitely extended crystal can emerge. They uniquely identify the IC state and can be used to image IC

domains and separate them from any coexisting commensurate domains. Here, IC domains go beyond the established concept of ferroic domains because in contrast to commensurate translation domains neighboring IC domains differ by a lattice translation that exceeds the boundary of a single unit cell.[27]

From the point of view of application we have characterized SHG as a tool for studying the properties of coexisting commensurate and IC forms of order in a single experiment. The local symmetry reduction in an IC crystal leads directly to the manifestation of additional, "hidden" degrees of freedom for forming domains that are accessible by SHG. These additional degrees of freedom play an important role for the manifestation of the functionalities of materials with IC order. For instance, in multiferroic $MnWO_4$ the correlation between the magnetically ordered IC state and its domains on the one hand and the commensurate dielectric properties of the material on the other hand is a key for understanding the complex magnetoelectric interactions of the crystal.

ACKNOWLEDGMENTS

This work was supported by the DFG through the SFB608. The authors thank Pierre Tolédano for many fruitful discussions about the Landau theory of incommensurate structures.

[1] W. Steurer and T. Haibach, in *International Tables for Crystallography*, edited by U. Shmueli (Springer, Dodrecht, 2008), Vol. B, Chap. 4.
[2] U. Dehlinger, Z. Kristallogr. **65**, 615 (1927).
[3] D. Shechtman, I. Blech, D. Gratias, and J. W. Cahn, Phys. Rev. Lett. **53**, 1951 (1984).
[4] E. Fontes, P. A. Heiney, and W. H. de Jeu, Phys. Rev. Lett. **61**, 1202 (1988).
[5] M. B. Salamon, S. Sinha, J. J. Rhyne, J. E. Cunningham, R. W. Erwin, J. Borchers, and C. P. Flynn, Phys. Rev. Lett. **56**, 259 (1986).
[6] P. L. Taylor and A. Banerjea, Ferroelectrics **66**, 135 (1986).
[7] B. O. Wells, Y. S. Lee, M. A. Kastner, R. J. Christianson, R. J. Birgeneau, K. Yamada, Y. Endoh, and G. Shirane, Science **277**, 1067 (1997).
[8] C. H. Chen and S.-W. Cheong, Phys. Rev. Lett. **76**, 4042 (1996).
[9] A. B. Harris and G. Lawes, in *Handbook of Magnetism and Advanced Magnetic Materials*, edited by H. Kronmüller and S. Parkin (Wiley, New York, 2005), Vol. 5.
[10] B. Toudic, P. Garcia, C. Odin, P. Rabiller, C. Ecolivet, E. Collet, P. Bourges, G. J. McIntyre, M. D. Hollingsworth, and T. Breczewski, Science **319**, 69 (2008).
[11] H. Katsura, N. Nagaosa, and A. V. Balatsky, Phys. Rev. Lett. **95**, 057205 (2005).
[12] M. Mostovoy, Phys. Rev. Lett. **96**, 067601 (2006).
[13] I. A. Sergienko and E. Dagotto, Phys. Rev. B **73**, 094434 (2006).
[14] P. M. de Wolff, Acta Crystallogr., Sect. A: Cryst. Phys., Diffr., Theor. Gen. Crystallogr. **30**, 777 (1974).
[15] J. C. Tolédano and P. Tolédano, *The Landau Theory of Phase Transitions* (World Scientific, Singapore, 1987).
[16] M. Fiebig, V. V. Pavlov, and R. V. Pisarev, J. Opt. Soc. Am. B **22**, 96 (2005).
[17] Th. Rasing, J. Magn. Magn. Mater. **175**, 35 (1997).
[18] Y. Uesu, S. Kurimura, and Y. Yamamoto, Appl. Phys. Lett. **66**, 2165 (1995).
[19] M. Fiebig, Th. Lottermoser, D. Fröhlich, A. V. Goltsev, and R. V. Pisarev, Nature (London) **419**, 818 (2002).
[20] H. Regensburger, R. Vollmer, and J. Kirschner, Phys. Rev. B **61**, 14716 (2000).
[21] M. Fiebig, N. P. Duong, T. Satoh, B. B. Van Aken, K. Miyano, Y. Tomioka, and Y. Tokura, J. Phys. D **41**, 164005 (2008).
[22] V. V. Lemanov, Ferroelectrics **117**, 93 (1991).
[23] T. D. Ibragimov and I. I. Aslanov, Solid State Commun. **123**, 339 (2002).
[24] Y. Qin, Y. Zhu, S. Zhu, and N. Ming, J. Appl. Phys. **84**, 6911 (1998).
[25] V. A. Golovko and A. I. Levanyuk, JETP Lett. **32**, 94 (1980).
[26] D. Meier, M. Maringer, Th. Lottermoser, P. Becker, L. Bohatý, and M. Fiebig, Phys. Rev. Lett. **102**, 107202 (2009).
[27] D. Meier, N. Leo, Th. Lottermoser, P. Becker, L. Bohatý, and M. Fiebig, Mater. Res. Soc. Symp. Proc. **1199**, 1199-F02-07 (2010); D. Meier, N. Leo, T. Jungk, E. Soergel, P. Becker, L. Bohatý, and M. Fiebig, arXiv:1008.3290 (unpublished).
[28] D. Meier, N. Leo, M. Maringer, Th. Lottermoser, M. Fiebig, P. Becker, and L. Bohatý, Phys. Rev. B **80**, 224420 (2009).
[29] M. Kenzelmann, A. B. Harris, S. Jonas, C. Broholm, J. Schefer, S. B. Kim, C. L. Zhang, S.-W. Cheong, O. P. Vajk, and J. W. Lynn, Phys. Rev. Lett. **95**, 087206 (2005).
[30] T. Kimura, Y. Sekio, H. Nakamura, T. Siegrist, and A. P. Ramirez, Nature Mater. **7**, 291 (2010).
[31] G. Lawes, A. B. Harris, T. Kimura, N. Rogado, R. J. Cava, A. Aharony, O. Entin-Wohlman, T. Yildrim, M. Kenzelmann, C. Broholm, and A. P. Ramirez, Phys. Rev. Lett. **95**, 087205 (2005).
[32] G. Lautenschläger, H. Weitzel, T. Vogt, R. Hock, A. Böhm, M. Bonnet, and H. Fuess, Phys. Rev. B **48**, 6087 (1993).
[33] P. Tolédano, B. Mettout, W. Schranz, and G. Krexner, J. Phys.: Condens. Matter **22**, 065901 (2010).
[34] A. B. Harris, Phys. Rev. B **76**, 054447 (2007).
[35] A. H. Arkenbout, T. T. M. Palstra, T. Siegrist, and T. Kimura, Phys. Rev. B **74**, 184431 (2006).
[36] K. Taniguchi, N. Abe, T. Takenobu, Y. Iwasa, and T. Arima, Phys. Rev. Lett. **97**, 097203 (2006).
[37] The Cartesian system $(\mathbf{x},\mathbf{y},\mathbf{z})$ is related to the monoclinic crystallographic system (with a=4.830 Å, b=5.7603 Å, c=4.994 Å, and β=91.14°) as follows: $\mathbf{y}=\mathbf{b}/b$, $\mathbf{z}=\mathbf{c}/c$, and $\mathbf{x}=\mathbf{y}\times\mathbf{z}$.
[38] R. W. Boyd, *Nonlinear Optics* (Academic Press, London, 2008).
[39] R. R. Birss, *Symmetry and Magnetism* (North-Holland, Amsterdam, 1966).
[40] P. Becker, L. Bohatý, H. J. Eichler, H. Rhee, and A. A. Kaminskii, Laser Phys. Lett. **4**, 884 (2007).
[41] A. Nogami, T. Suzuki, and T. Katsufuji, J. Phys. Soc. Jpn. **77**, 115001 (2008).

[42] K. Taniguchi, M. Saito, and T. H. Arima, Phys. Rev. B **81**, 064406 (2010).
[43] D. R. Huffman, R. L. Wild, and M. Shinmei, J. Chem. Phys. **50**, 4092 (1969).
[44] V. Dvorák, V. Janovec, and Y. Ishibashi, J. Phys. Soc. Jpn. **52**, 2053 (1983).
[45] T. Finger, D. Senff, K. Schmalzl, W. Schmidt, L. P. Regnault, P. Becker, L. Bohatý, and M. Braden, Phys. Rev. B **81**, 054430 (2010).
[46] W. S. Choi, K. Taniguchi, S. J. Moon, S. S. A. Seo, T. Arima, H. Hoang, I.-S. Yang, T. W. Noh, and Y. S. Lee, Phys. Rev. B **81**, 205111 (2010).
[47] P. Lehnen, J. Dec, W. Kleemann, Th. Woike, and R. Pankrath, Ferroelectrics **240**, 1547 (2000).
[48] M. Pavel, I. Rychetský, and P. Petzelt, J. Appl. Phys. **89**, 5036 (2001).